

levels. It could do so by stimulation of adenylyl cyclase activity, or, as suggested elsewhere (15), by an inhibition of cyclic AMP phosphodiesterase activity. It would appear that Ca^{2+} must play a role in regulating the activity of one of these two enzymes, since Ca^{2+} is not required for cyclic AMP-stimulated melanosome dispersion. The Ca^{2+} requirement for MSH action on melanophores is consistent with a similar cation requirement for the lipolytic action of adrenocorticotrophic hormone (ACTH) on isolated fat cells (16) or the stimulation of adenylyl cyclase activity in adrenal cortical microsomal fractions (17). The similarity in structure of these two hormones might suggest a similar mechanism of action.

DAVID L. VESELY

Department of Biological Sciences
and College of Medicine,
University of Arizona,
Tucson 85721

MAC E. HADLEY

Department of Biological Sciences,
University of Arizona

Endothelial Projections as Revealed by Scanning Electron Microscopy

Abstract. Scanning electron micrographs of the endothelium of the pulmonary artery reveal that the entire surface is covered by a meshwork of irregular projections which vastly increase the surface area. The size and density of the projections suggest that they may function to direct an eddying flow of plasma along the endothelial surface.

The endothelial lining of blood vessels is remarkable not only for its extensiveness and thinness but also for its position in direct communication with blood. Previous studies of the structure and function of endothelium have concentrated on the selective transport of fluid and solutes in capillaries, the structural studies having focused on cell junctions, pinocytotic vesicles, and endothelial flaps (1). Recent evidence indicates that enzymes on or near the surface of endothelial cells are actively engaged in the metabolism of circulating substances, such as the adenine nucleotides and polypeptide hormones,

which are degraded rapidly but which are not retained by the cell itself (2).

Observation of the endothelial surface by scanning electron microscopy emphasizes a very different aspect which has been overlooked in transmission electron micrographs. The surface is covered by a profuse array of minute, irregular, fingerlike projections. The projections are distinguished from the regular palisades of microvilli which are characteristic of many vertebrate and invertebrate epithelia and from flaps or marginal folds.

Figures 1 and 2A show the inner surface of the pulmonary artery of a

References and Notes

1. K. Shizume, A. B. Lerner, T. B. Fitzpatrick, *Endocrinology* **54**, 533 (1954); A. B. Lerner, *Nature* **184**, 674 (1959).
2. A. B. Lerner and J. D. Case, *J. Invest. Dermatol.* **32**, 211 (1959); A. B. Lerner and J. S. McGuire, *Nature* **189**, 176 (1961); R. S. Snell, *J. Invest. Dermatol.* **42**, 337 (1964); M. E. Hadley and W. C. Quevedo, Jr., *Nature* **209**, 1334 (1966).
3. R. R. Novales, *Physiol. Zool.* **32**, 15 (1959).
- 3a. ———, B. J. Novales, S. H. Zinner, J. A. Stoner, *Gen. Comp. Endocrinol.* **2**, 286 (1962).
4. S. Dikstein, C. P. Weller, F. G. Sulman, *Nature* **200**, 1106 (1963).
5. M. Fingerman, *Amer. Zool.* **9**, 443 (1969).
6. S. B. Horowitz, *J. Cell. Comp. Physiol.* **51**, 341 (1958).
7. J. M. Goldman and M. E. Hadley, *J. Pharmacol. Exp. Therap.* **166**, 1 (1969).
8. K. Abe, R. W. Butcher, W. E. Nicholson, C. E. Baird, R. A. Liddle, G. W. Liddle, *Endocrinology* **84**, 362 (1969).
9. E. W. Sutherland, I. Øye, R. W. Butcher, *Recent Progr. Horm. Res.* **21**, 623 (1965).
10. M. W. Bitensky and S. R. Burstein, *Nature* **208**, 1282 (1965); R. R. Novales and W. J. Davis, *Endocrinology* **81**, 283 (1967); R. R. Novales and W. J. Davis, *Amer. Zool.* **9**, 479 (1969); J. T. Bagnara and M. E. Hadley, *ibid.* **9**, 465 (1969).
11. J. M. Goldman and M. E. Hadley, *Gen. Comp. Endocrinol.* **13**, 151 (1969).
12. M. E. Hadley and J. M. Goldman, *Amer. Zool.* **9**, 489 (1969).
13. ———, *Brit. J. Pharmacol.* **37**, 650 (1969).
14. E. W. Sutherland and T. W. Rall, *J. Biol. Chem.* **232**, 1077 (1958); R. W. Butcher and E. W. Sutherland, *ibid.* **237**, 1244 (1962).
15. J. M. Goldman and M. E. Hadley, *Brit. J. Pharmacol.* **39**, 160 (1970); J. M. Goldman and M. E. Hadley, *Eur. J. Pharmacol.* **12**, 365 (1970).
16. E. Lopez, J. E. White, F. L. Engel, *J. Biol. Chem.* **234**, 2254 (1959); J. F. Kuo, *Biochim. Biophys. Acta* **208**, 509 (1970).
17. H.-P. Bär and O. Hechter, *Biochem. Biophys. Res. Commun.* **35**, 681 (1969).
18. Supported by NSF grant GB 8347, and a biomedical sciences support grant FR 07002 from the General Research Resources, Bureau of Health Professions Education and Manpower Training, NIH.

17 May 1971

3 SEPTEMBER 1971

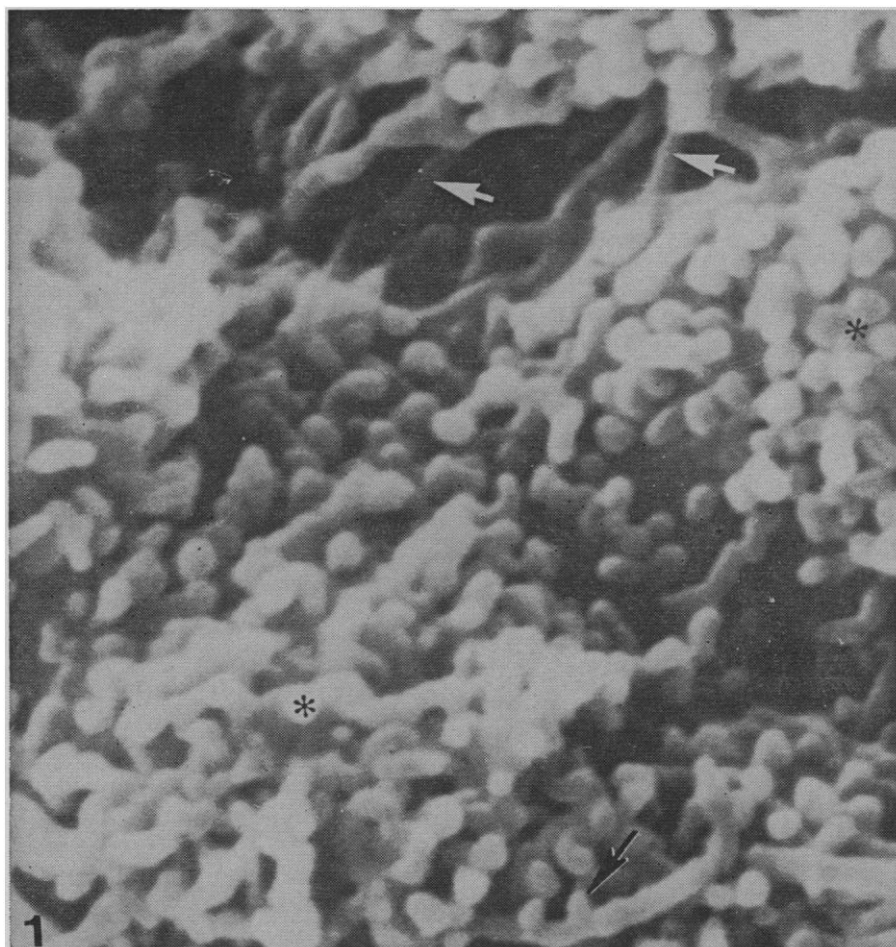


Fig. 1. Scanning electron micrograph. The endothelial projections are approximately 250 to 350 nm in diameter and vary in length from 300 to 3000 nm. They may take the form of knobs or longer arms, some of which branch or bud (black arrow). They are densest over the main body of the cell (*) but extend laterally to overlap adjacent cells (white arrows) ($\times 14,000$).

dog examined by scanning electron microscopy (3). The lining is thrown into a series of projections which occur over the entire surface of each endothelial cell. Reference to thin sections in the transmission electron microscope confirms the presence of these projections (Fig. 2, B and C), but their

numerical prominence and functional importance can only be appreciated in a three-dimensional scanning survey of the entire surface.

The projections are approximately 250 to 350 nm in diameter and 300 to at least 3000 nm long, as estimated from the scanning electron micro-

graphs. Some of the shorter projections come to blunt ends whereas others end in knoblike processes. Longer projections may bud or branch. The branches may occasionally fuse with other projections or with the main surface of the cell. Measurements of the diameters of the projections are in good agreement, as estimated from the transmission and from the scanning electron micrographs.

The projections contain pinocytotic vesicles and ribosomes (Fig. 2, B and C). Mitochondria are situated at the base of some. Fibrillar structures are evident in the body of the cell, especially beneath the nucleus (4), and may extend to the base of the projections (Fig. 2C).

The projections occur in concentrations of up to seven per square micrometer (Fig. 1). The denser clusters are found over the body of the cell. Numbers become smaller near cell junctions. Projections near cell junctions extend toward, and intertwine with, the adjacent cell, but we have no evidence of the fusion of a projection of one cell with that of another.

The long axis of some projections may parallel the main surface of the cell. Both the density of the clusters and the tendency of long branches to reflect back on the main surface of the cell would appear to make it unlikely that formed elements of blood could come in contact with the body of the cell.

Although our scanning electron microscopic studies of endothelial surface projections are limited to the lining of the pulmonary artery of the dog, transmission micrographs indicate that these structures occur in much smaller vessels of a wide number of species and are a general feature of the intima of blood vessels. The projections may be similar to the surface specializations in the vessels of the pecten of the bird's eye (5) and to endothelial microvilli in the vessels of the rat Gasserian ganglion and testis (6). In addition, published transmission electron micrographs (7) of capillaries of the pancreas (cat) and myocardium (mouse) and unpublished micrographs of capillaries in lung (rat) (8) show projections arising from the main body of the endothelial cell; circular structures within the lumen are presumably transverse sections of endothelial projections.

The low-power scanning electron micrograph shows projections over the entire endothelial surface and no preferential localization at the periphery of

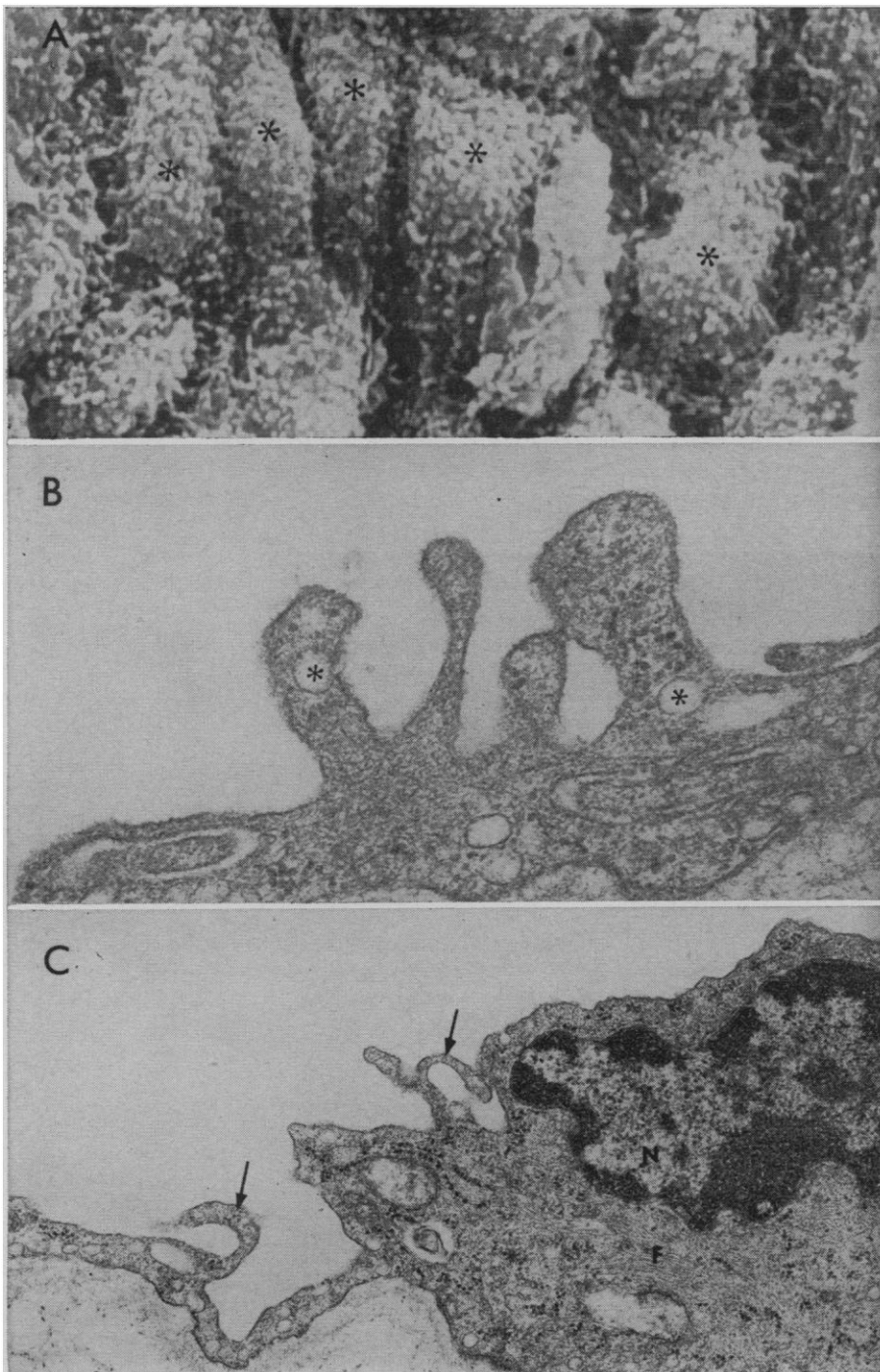


Fig. 2. (A) Low-power scanning electron micrograph of the inner surface of the dog pulmonary artery. The endothelial cells are denoted by an asterisk, the cell outlines being clearly distinguishable. The main body of each endothelial cell is richly covered by an array of irregular projections which thin out toward the borders of the cell ($\times 3000$). (B) Detail of a group of endothelial projections showing the apparent variability in diameter. Note pinocytotic vesicles (asterisk) associated with the projections ($\times 75,000$). (C) Portion of an endothelial cell with nucleus (N). Fibrillar strands (F) are present in the subnuclear cytoplasm. Endothelial projections (arrows) occur both on the main body of the cell and on the tenuous peripheral portions ($\times 29,000$).

the cell. While marginal folds may occur in addition, the structures which we describe here and which we have compared by scanning and transmission electron microscopy are not folds but rather projections with a circular profile in transverse section. It is unlikely that these fingerlike projections function in conjunction with the process of pinocytosis by engulfing plasma as suggested for the marginal folds (1). Although the projections may reflect onto and fuse with the main body of the cell, their cylindrical shape would make them no more efficient than an apposed thumb and forefinger for holding water. On the other hand, the projections could possibly enmesh small chylomicra.

The functions of the endothelial surface projections are not known. Clearly, the projections vastly increase the surface area of endothelial cells and cannot fail to affect fluid dynamics. Their density and the irregular meshwork which they form are such that they could have the effect of producing an eddying flow of cell-free plasma along the surface of the cell body. This possibility is of special interest in relation to large vessels with a high flow such as the pulmonary artery, where nutrient capillaries enter the adventitia and outer media but do not penetrate to the endothelium. A retarded flow of plasma along the surface of the cell could provide conditions of flow and pressure favorable for the exchange of metabolites and, possibly, for the metabolism of circulating hormones.

UNA SMITH
JAMES W. RYAN

Department of Medicine,
University of Miami, and Howard
Hughes Medical Institute,
Miami, Florida 33152

DAVID D. MICHIE
Division of Thoracic and
Cardiovascular Surgery,
University of Miami School of
Medicine, Miami, Florida 33152

DAVID S. SMITH
Department of Medicine,
University of Miami, and
Papanicolaou Cancer Research
Institute, Miami, Florida 33152

References and Notes

1. D. W. Fawcett, *The Cell* (Saunders, Philadelphia, 1966), p. 394; G. Majno, *Handbook of Physiology* (American Physiological Society, Washington, D.C., 1965), vol. 3, p. 2293; G. E. Palade, *Anat. Rec.* **136**, 254 (1960).
2. J. W. Ryan, J. Roblero, J. M. Stewart, *Adv. Exp. Med. Biol.* **8**, 263 (1970); *Biochem. J.* **110**, 795 (1968); —, W. P. Leary, *Chest* **59**, 8S (1971); J. W. Ryan, J. M. Stewart, W. P. Leary, J. G. Ledingham, *Biochem. J.* **120**, 221 (1970); U. Smith and J. W. Ryan, *Pharmacol. Res. Commun.* **1**, 197 (1969); *Adv. Exp. Med. Biol.* **8**, 249 (1970a); *J. Cell Biol.* **47**, 196a (1970b); *Chest* **59**, 12S (1971).

3. Dogs were anesthetized with sodium pentobarbital (25 mg per kilogram of body weight) administered intravenously. A portion of the pulmonary artery near the pulmonary valve was removed, immediately dropped into 0.25M glutaraldehyde in 0.05M cacodylate buffer (pH 7.4) containing 0.17M sucrose, and prepared for transmission electron microscopy. For scanning electron microscopy, material was transferred from the cacodylate buffer to 1 percent O₂O₁ in the same buffer. The small tissue blocks were frozen in liquid Freon 12 cooled by liquid nitrogen and dehydrated under vacuum. The specimens were then attached to glass cover slips with the luminal surface of the endothelium uppermost. The material was shadowed by evaporation of a gold and platinum alloy on the surface and examined in a Philips AMR 900 microscope.
4. G. Majno, S. M. Shea, M. Leventhal; *J. Cell Biol.* **42**, 647 (1969).

5. D. W. Fawcett, in *The Peripheral Blood Vessels*, J. L. Orbison and D. E. Smith, Eds. (Williams & Wilkins, Baltimore, 1963), p. 17.
6. G. Gabbiani and G. Majno, *Z. Zellforsch. Mikrosk. Anat.* **97**, 111 (1969).
7. W. Bloom and D. W. Fawcett, *A Textbook of Histology* (Saunders, Philadelphia, 1968), p. 358; R. S. Cotran, in *Physical Basis of Circulatory Transport*, E. B. Reeve and A. C. Guyton, Eds. (Saunders, Philadelphia, 1967), p. 249.
8. U. Smith and J. W. Ryan, unpublished micrographs.
9. Supported by the Florida Heart Association, PHS research grant HE 12843, NSF grant GB-12117X, and the Council for Tobacco Research. We thank Dr. S. B. Moll, Advanced Metals Research, Inc., Burlington, Massachusetts, for taking the scanning electron micrographs, and Research Division, Electron Microscopy Laboratory, Veterans Administration Hospital, Miami, Florida, for use of the Philips EM 300.

12 July 1971

Plasmalemma: The Seat of Dual Mechanisms of Ion Absorption in *Chlorella pyrenoidosa*

Abstract. *Dual mechanisms of absorption of rubidium were demonstrated in a nonvacuolate unicellular alga, Chlorella pyrenoidosa, in both the light and the dark. The two mechanisms were sensitive to metabolic inhibitors. At high concentrations rubidium enhanced the respiration of Chlorella cells. The findings support the conclusion that the mechanisms of rubidium absorption in both the low and high concentration ranges are active processes and reside in the plasmalemma.*

Epstein *et al.* (1) discovered that the rate of ion absorption by plant cells followed two distinct patterns possibly due to two different mechanisms, one operating over a concentration range of the ion up to 1 mM, and the other extending from 1 mM upward. Later, a theory proposed by Laties and his co-workers (2, 3) suggested that the first mechanism is located at the plasmalemma and the second at the tonoplast. It is further held that ions in the high concentration range enter the plasmalemma by diffusion. However, this theory has been questioned by others (4-6) who hold that both mechanisms are located in the plasmalemma and operate in parallel. Welch and Epstein (6) consider that the Laties theory contradicts the classical view of the semipermeability and ion selectivity properties of the plasma membrane.

Dual patterns of absorption have been recorded for a number of ions in tissues of several higher plants (4, 7) and for carbohydrate in microorganisms (8). Studies made so far with *Chlorella pyrenoidosa* relate to the membrane potentials and the kinetics of potassium influx (9, 10). Dual patterns of rubidium absorption in *C. pyrenoidosa* are reported here. It is further demonstrated that both mechanisms reside in the plasmalemma and that absorption of rubidium in the high concentration range (1 to 50 mM) is metabolically mediated.

The alga *C. pyrenoidosa* was grown in aerated nutrient culture (11) at 20°C, under 5000 lu/m² of fluorescent light. The cells were washed thrice with deionized distilled water before use. The procedures for incubation and measurement of ion absorption were those

Table 1. Effects of metabolic inhibitors on rubidium absorption by *Chlorella* cells from 0.2 and 10 mM RbCl in the light and the dark. The inhibitors (10⁻⁶M) were presented along with RbCl. Values are means ± standard errors of the means.

Treatment	Rubidium absorption (nmole/mg per hour)			
	0.2 mM RbCl		10 mM RbCl	
	Light	Dark	Light	Dark
Control	25.5 ± 0.4	9.5 ± 0.1	37.0 ± 2.8	23.1 ± 0.9
Antimycin A	12.7 ± .8	2.5 ± .3	28.8 ± 1.2	8.0 ± .9
m-Cl-CCP	21.2 ± 1.2	7.6 ± .6	29.8 ± 1.1	15.3 ± .1
p-CF ₃ O-CCP	21.5 ± 0.6	7.9 ± .7	30.1 ± 1.8	14.5 ± .1